COMPDYN 2017
6th ECCOMAS Thematic Conference on
Computational Methods in Structural Dynamics and Earthquake Engineering
M. Papadrakakis, M. Fragiadakis (eds.)
Rhodes Island, Greece, 15–17 June 2017

A MECHANISTIC APPROACH IN DEFINING INELASTIC ROTATION CAPACITY OF RC COLUMNS

Konstantinos G. Megalooikonomou[1], Stavroula J. Pantazopoulou[2], and Souzana P. Tastani[3]

[1] Department of Civil and Environmental Engineering, University of Cyprus, P.O. Box 20537, 1687 Nicosia, Cyprus, kmegal01@ucy.ac.cy

[2]The Lassonde Faculty of Engrg., York University, 4700 Keele St, Toronto ON. M3J 1P3, Canada
pantazo@yorku.ca

[3]Democritus University of Thrace, Kimmeria Campus, Building B, Xanthi 67100, Greece
stastani@civil.duth.gr

Keywords: Shear Span, Bond, Yield-Penetration, Plastic Hinge Length, Inelastic Rotation.

Abstract. *When a reinforced concrete (RC) column is subjected to lateral sway as a result of earthquake action, the large strain demand in the end sections is supported by development of strains in the anchorage. This causes the bars to displace (or slip) relative to the anchoring concrete at the column fixed end(s). The lumped slip causes rigid-body rotation of the column, thereby alleviating partially the column deformation. This reinforcement slip is assumed to occur in the tension bars only and cause the rotation about the neutral axis. Development of flexural yielding and large rotation ductilities in the plastic hinge zones of frame members is synonymous with the spread of bar reinforcement yielding. Yield penetration in the anchored reinforcing bar inside the shear span of the column where it occurs, destroys interfacial bond between bar and concrete and reduces the strain development capacity of the reinforcement. This affects the plastic rotation of the member by increasing the contribution of bar slippage. In order to establish the plastic rotation in a manner consistent with the above definition, this paper uses the explicit solution of the field equations of bond over the shear span of a column. Through this approach, the bar strain distributions and the extent of yield penetration from the yielding cross section towards the shear span are resolved and calculated analytically. By obtaining this solution the aim is to illustrate the true parametric sensitivities of plastic hinge length as a design variable for practical use in seismic assessment of existing structures. Results obtained from the analytical procedures are compared with experimental evidence from tests conducted on reinforced concrete columns under seismic loading reported in the literature.*

1. INTRODUCTION

Pullout rotation accounts for a significant fraction of the deformation capacity of reinforced concrete (RC) columns. It occurs in the critical sections near the end supports as a result of the penetration of strains both inside the support of the member (*e.g.* footing) but also inside the shear span. In columns that do not fail by web crushing, strains spread further into the anchorage gradually with increasing applied chord rotation, claiming a predominant share of the members' deformation capacity near the ultimate limit state. This aspect of the response is evaluated from estimation of reinforcement slip; slip may be estimated approximately or it may be evaluated from solution of the field equations of bond along the principal reinforcement of the column as it sways laterally. Slip of the bars occurs where large inelastic strains may develop – i.e. in the yield penetration length over the anchorage and in the plastic hinge zone in the shear span. The kinematics of the pullout slip are accompanied by, (a) vertical displacement which is reported to occur at the tip of the cantilever column during cycling under lateral loading (b) acceleration of crushing of the concrete cover in the compression zone due to the local increase in compression strains [1].

Degradation of bond - beyond a critical slip value that marks the initiation of the descending branch in the local bond-slip law causes spreading of strains away from the critical section so that a larger fraction of the bar is eventually exposed to large strains. Analytical models representing the state of bond along the lateral surface of an embedded reinforcing bar are intended for interpretation and simulation/prediction of the behavior of structural concrete in a manner consistent with first principles. Previous studies have illustrated how detailed bond models may be used in the study of stress states arising in the assessment of the rotation capacity of RC members [2]. Through evaluation of the strain distribution it is possible to estimate the localization of excessive strain magnitudes in the critical zones, thereby enabling a novel approach for evaluation of the plastic hinge length in flexure-shear members. Additionally, the reinforcement stress and strain response and its displacement with respect to the surrounding concrete can be explicitly described through the solution of the equations of bond in the shear span of the member; this enables a detailed study of the tension stiffening phenomena, and how these affect the behavior of cracked concrete.

In this paper, a unidirectional model of bond is considered as a basis for the evaluation of the longitudinal strain distribution of the primary reinforcement of the column. Although several solutions that refer to the problem of force development along the anchorage have been proposed, yet the problem of strain penetration in the anchorage has received limited attention from researchers [3, 4]. Related studies have been conducted for lap splices developed in a region of constant moment (no shear) [5]. On the other hand, the problem of strain penetration in the shear span of the member has not been addressed explicitly yet.

2. CONSTITUTIVE RELATIONSHIPS FOR BAR TO CONCRETE BOND

The basic equations that describe force transfer lengthwise from a bar to the surrounding concrete through bond are derived from force equilibrium applied to an elementary bar segment of length dx and from compatibility between bar translation (slip), axial bar strain ε, and concrete strain ε_c over dx, namely [6,7]:

$$df/dx = -(4/D_b)f_b\ ,\ ds/dx = -(\varepsilon - \varepsilon_c) \cong -\varepsilon \tag{1}$$

where f is the axial stress of the bar; D_b is the bar diameter ; f_b is the local bond stress and s is the relative slip of the bar with respect to the surrounding concrete. The terms in Eq. (1) are related through the bond-slip law, $f_b = f_b(s)$ and the bar material stress-strain relationship,

$f=f(\varepsilon)$. The concrete contribution to relative slip is $\varepsilon_c dx$; this term is neglected when dealing with normal-weight concrete, considering that the average concrete strain is an order of magnitude smaller than the average bar strain. Solution of Eq. (1) is possible though exact integration, resulting in closed-form solutions for the state of stress and strain along the anchorage, through pertinent selection of simple models for the material laws (*e.g.* piecewise linear relations). This approach has a clear advantage over the numerical solution alternative in that it enables transparent insight into the role of the various design parameters on the behavior of bar anchorages.

Solution of Eq. (1) requires that the general form of the constitutive relationships of the bar and the local bond-slip law are known (Fig. 1). Here the reinforcing bar stress-strain relationship is considered elastoplastic with hardening (representing conventional steel reinforcement) (Fig. 1a). Without loss of generality, and to facilitate derivation of closed-form solutions, a linear elastic, perfectly plastic local bond-slip relationship with residual bond is assumed. The last branch represents the residual friction between the concrete cover and the steel bar after failure of the rib interlocking mechanism (Fig. 1b). The plateau in the local bond-slip law implies sustained bond strength. This feature is not always manifested in the test data; to be measured it requires redundancy in the anchorage (i.e., availability of longer anchorages to enable force redistribution before failure). In the assumed law the end of the plateau is marked by abrupt loss of bond strength to a residual value f_b^{res}. (Note that f_b^{res} is taken nonzero only in the case of ribbed steel bars, but not for smooth steel bars.)

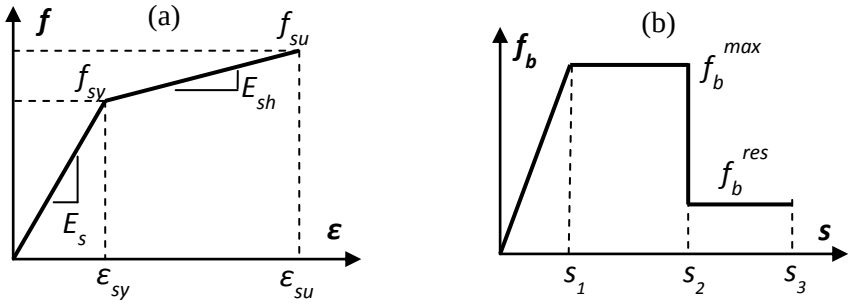

Figure 1: (a) Stress-strain law of steel bar and (b) local bond law

3. TENSION-STIFFENING MODEL

It was mentioned earlier that spread of inelastic strains occurs on both sides of a critical section (*e.g.* at the base of a column). The process of inelastic strain penetration in the anchorage of a reinforcing bar has already been demonstrated in [8]. This section is dedicated to solving the same problem in the other side of the critical section, that is, along the shear span of a column. Here the problem is different from that of the anchorage only in the type of boundary conditions that may be enforced (in other words, the governing differential equation is the same); with regards to the bond-slip law, although the general form of the multilinear envelope may be taken the same, the bond strength value, f_b^{max}, may be less in the shear span as compared to the anchorage due to the reduced confinement available. Considering the column under lateral sway, the moment-shear relationship in the span of a cantilever RC column under horizontal loading is identical to that occurring over the length of the actual frame member extending from the inflection point at midheight (this is the point of zero moment, zero curvature) to the fixed end support.

Before any kind of cracking takes place along the length of the flexural member, the bar strain is estimated from the flexural analysis of the uncracked column cross section *(i.e.* the

moment-curvature analysis) as per the Eq. (2) where $M(x)$ is the moment at distance x from the support, E is the elastic modulus of concrete, I_g is the moment of inertia of the uncracked section with area A (referred to as gross section), N is the axial load, h is the section height and c is the cover (Fig. 2a):

$$\varepsilon(x) = \left(M(x) \cdot y_{s.na} / \left(E \cdot I_g\right)\right) - N/(E \cdot A)\ ,\ y_{s.na} = (h/2) - c - 0.5D_b \tag{2}$$

$$\text{or more generally: } \varepsilon(x) = \varphi(x) \cdot y_{s.na} \tag{3}$$

with $y_{s.na}$ the distance from the neutral axis to the centroid of tension reinforcement (Fig. 2a), and $\varphi(x)$ the curvature on the cross section at distance x from the support. The distance to the neutral axis changes significantly from the initial linear elastic state $y_{s.na}^{gr}$, to the cracked state of a cross section $y_{s.na}^{cr}$. If the concrete tension zone of the member is uncracked, the position of the neutral axis may be estimated from equilibrium requirements; same holds in locations where distinct cracks have formed if it may be assumed that "plane sections remain plane". Based on classical flexural analysis concepts, a RC member may be considered "cracked" in regions where the flexural moment exceeds the cracking moment. Although a large region may satisfy this definition, however, cracks occur at discrete locations x_{icr}. Thus, if an analysis of the cracked cross section is available, the reinforcement strains $\varepsilon(x_{icr})$ that occur in the crack locations may be calculated from Eq. (3). However, it is clear that in the segment between cracks, where moment may exceed the cracking value, bar strains cannot be estimated from flexural analysis as prescribed by Eq. (3). The reason is that due to reinforcement slip, the degree of strain compatibility between steel and concrete in these locations is not well understood, as would be required by the "plane-sections remain plane" assumption, nor can the concrete be considered inert as would happen in a fully cracked tension zone. Because it takes some distance from a crack location before the reinforcement may fully engage its concrete cover in tension so as to satisfy the conditions of strain compatibility, it is clear that Eq. (3) may be invalid even in regions adjacent to a flexural crack, even if the moment in these regions falls below the cracking limit. The bar strain in these regions may be estimated from solution of the differential equation of bond. To address all the possible exceptions to the validity of the flexural requirement stated by Eqs. (2,3), here the term "undisturbed" is used as a qualifier to "uncracked" in order to refer to sections that satisfy the plane sections remain plane compatibility requirement, where concrete and reinforcement strains at the same

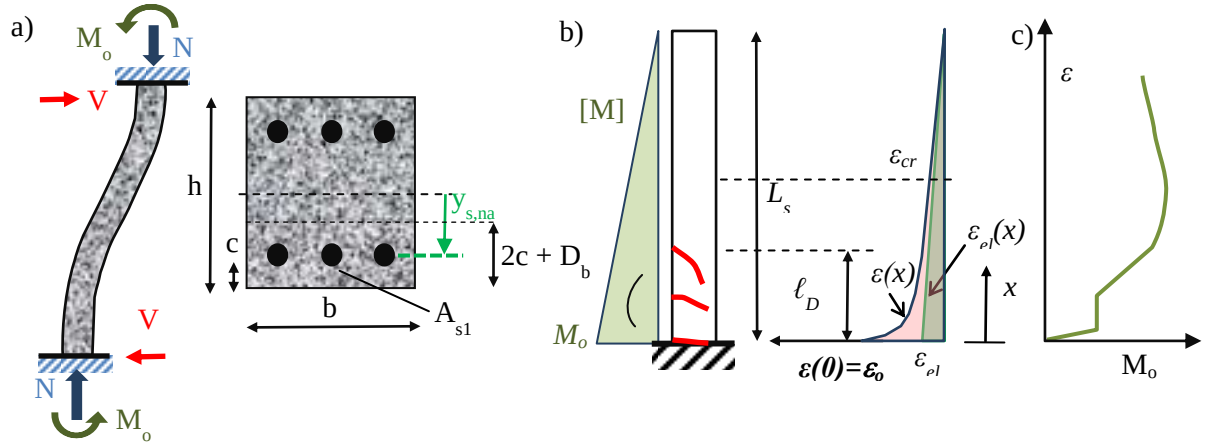

Figure 2: a) Definition of terms for lateral sway. b) Moment distribution along the shear span L_s and definition of disturbed region, l_D. c) The bar strain at the critical section experiences a significant jump upon cracking even though the moment from the uncracked to the cracked stage may be imperceptible.

distance from the neutral axis may be assumed equal. Thus, in regions where strains are ob-

tained from solution of the bond equation, this requirement is not valid – therefore even if apparently uncracked, the region may be "disturbed" according with this definition.

The length of shear span is referred to henceforth as L_s. The flexural moment in any cross section x (Fig. 2b), where x is measured from the face of the support, may be obtained from equilibrium with reference to the flexural moment occurring at the support, M_o (ε_o is the corresponding steel strain), according with:

$$\mathrm{M(x)} = \mathrm{M_0} \cdot (1 - \mathrm{x/L_s}) \tag{4}$$

As the sequence of crack formation is critical for the occurrence of disturbed regions and for the problem of strain penetration that will be subsequently addressed, in the present discussion the static problem represented by Eq. (4) will be solved for a gradually increasing moment at the support. As a starting point in the following derivation, it is assumed that the characteristic flexural resistance curve of any cross section along the shear span (*i.e.* the moment – curvature and moment – bar strain diagram) are available from classical flexural analysis over the entire range of the response.

For a member with uniform primary reinforcement over its length, the moment distribution that follows Eq. (4) will cause first cracking at the face of the support. According with the preceding discussion, the bar strain at the base of a cantilever column with shear span L_s experiences a significant jump upon cracking of the tension zone to maintain equilibrium. For example, if the cracked section stiffness is about 1/3 of the uncracked value, the bar strain at the critical section is expected to increase threefold by the mere occurrence of the crack even though the moment change from the uncracked to the cracked stage may be imperceptible (Fig. 2c). Thus suddenly the whole region adjacent to the cracked location becomes "*disturbed*". Over the length of the disturbed region, the reinforcement strain is described by the solution of the bond equation [4] *i.e.*:

$$\varepsilon(\mathrm{x}) = \mathrm{C_1} \cdot \mathrm{e}^{-\omega \mathrm{x}} + \mathrm{C_2} \cdot \mathrm{e}^{\omega \mathrm{x}}, \quad \omega = [4 \mathrm{f_b^{max}}/(\mathrm{E_s} \cdot \mathrm{D_b} \cdot \mathrm{s_1})]^{0.5} \tag{5}$$

The solution of Eq. (5) is valid provided bond is in the elastic range (ascending branch in the bond slip law). Before the creation of any other crack, the disturbed region extends over a distance ℓ_D from the critical section. What characterizes the end of the disturbed region is that a) at that point the gradient of the bar strain distribution, $\psi = d\varepsilon(x)/dx$, obtained from Eq. (5), matches the slope of the strain diagram as would be obtained from the flexural analysis of the member, whereas b) the bar strain $\varepsilon(x)$ at that location satisfies simultaneously Eqs. (2,3,5). Therefore, from Eq. (4) it follows that the slope of the strain gradient owing to flexural moments at uncracked location ℓ_D is (Fig. 3):

$$\psi = \mathrm{d}\varepsilon(\mathrm{x})/\mathrm{dx} = -\left[\underbrace{\left(\mathrm{M_0} \cdot \mathrm{y_{s.na}^{gr}}\right)/\mathrm{EI_{gr}}}_{\varepsilon_{\mathrm{el}}}\right] \cdot 1/\mathrm{L_s} = \omega \cdot \left(-\mathrm{C_1} \cdot \mathrm{e}^{-\omega \ell_\mathrm{D}} + \mathrm{C_2} \cdot \mathrm{e}^{\omega \ell_\mathrm{D}}\right) \tag{6}$$

$$\varepsilon(\ell_\mathrm{D}) = \mathrm{C_1} \cdot \mathrm{e}^{-\omega \ell_\mathrm{D}} + \mathrm{C_2} \cdot \mathrm{e}^{\omega \ell_\mathrm{D}} = \varepsilon_{\mathrm{el}} \cdot (1 - \ell_\mathrm{D}/\mathrm{L_s}) - \mathrm{N}/(\mathrm{E} \cdot \mathrm{A}) \tag{7}$$

From the system of Eqs. (6, 7) the length of disturbed region adjacent to the crack may be determined if the moment at the support M_o is known. The solution given by Eq. (5) is also subject to the following boundary condition (Fig. 2b):

$$\varepsilon(0) = \mathrm{C_1} + \mathrm{C_2} = \varepsilon_\mathrm{o} \tag{8}$$

In an algorithm developed to solve Eq. (6,7,8) numerically, the controlling parameter is ε_o; therefore, at each incremental step which begins by selecting the value of ε_o, the corresponding moment M_o is uniquely determined from the moment- bar strain diagram of the member

cross section under study. Equations (6,7,8) are a system of three equations having three unknowns – given the value of ε_o and ω the unknowns are C_1, C_2 and ℓ_D. At this point it is relevant to determine the location of the next crack formation. Whether the next crack will form within the undisturbed or the disturbed region depends on the magnitude of tensile stress transferred through bond to concrete:

a) A check is performed regarding whether next cracking will occur in the disturbed region. The least value of coordinate $x< \ell_D$ should be determined that also satisfies the requirement:

$$[(E_s \cdot A_{s1})/(f_{ct} \cdot A_{c.eff})] \cdot [\varepsilon_o - \varepsilon(x)] = 1, \quad A_{c.eff} = b \cdot (2c + D_b) - A_{s1} \tag{9}$$

In Eq. (9) A_{s1} is the area of the tensile reinforcement, $A_{c.eff}$ is the area of concrete effectively engaged in tension, f_{ct} is the tensile concrete strength, b is the width of the section of the column (Fig. 2a). For a crack to be formed into ℓ_D the force undertaken by bond mechanism (i.e. $E_s A_{s1}[\varepsilon_o - \varepsilon(x)]$) should exceed the force of the effectively engaged in tension concrete (i.e. $f_{ct} A_{eff}$); in this case the left-hand expression of Eq. (9) should be >1 else no further cracking is possible in the disturbed zone as long as the reinforcement remains elastic.

b) A check is performed regarding whether next cracking will occur in the undisturbed region. Therefore the coordinate $x\geq \ell_D$ should be determined that satisfies the following requirement ($\varepsilon_{c.cr}$ is the cracking concrete strain) based on Eqs. (2,4):

$$\varepsilon(x) = \varepsilon_{el}(1 - x/L_s) - N/(E \cdot A) = \varepsilon_{c.cr} \Rightarrow x = L_s \cdot [1 - \varepsilon_{c.cr}/\varepsilon_{el} - N/(EA\,\varepsilon_{el})] \tag{10}$$

This process is repeated as the value of the strain ε_o in the support is increased. If the criterion (b) controls, *i.e.* the next crack forms in the undisturbed region, then from there on this becomes the controlling strain value and the next disturbed region that begins from that point and extends away from the support is calculated. The new disturbed region is defined for this crack, ℓ_{D2}; the total disturbed region of the cantilever extends from the support to the end of ℓ_{D2} beyond the second crack. This is denoted henceforth as ℓ_D (Fig. 3a). As the support strain increases this process is continued with more cracks forming towards the tip of the cantilever, with the disturbed region spreading further over the shear span. Its significance is that *over the total disturbed zone ℓ_D, bar strains are calculated from the solution of the bond equation, as in this region the assumption of plane-sections remaining plane is no longer valid.*

After stabilization of cracking (no more primary cracks develop) and beyond elasticity of the steel bar the yielded segment of the disturbed region undergoes simultaneous degradation of bond. Thus, of the total length ℓ_D, there is a segment l_r where yielding has penetrated (Fig. 3b). For that portion of the disturbed zone, bar strains increase without a commensurate increase of stress: this means that bond must have degraded to zero as a consequence of Eq. (1), since $df_s/dx=0$ and thus f_b=0. Even if the yield-plateau is neglected, and the bar stress-strain diagram is considered bilinear with hardening, it is clear that the small hardening slope may only be supported by the residual bond strength – in other words in order for a bar to yield, it must have slipped beyond the limit s_2 in the bond - slip law (Fig. 1). Note that limit s_2 is not an intrinsic property of the bar – concrete interface as several Codes define, rather it depends on the available bonded length [9].

Similar to the derivation of strain, slip and bond plastification for the yield penetration length of an elastoplastic bar in the anchorage [8], the following equations are defined for a yielded bar in a shear span. Since hardening is included in the steel's constitutive law a residual bond strength is obtained through the application of Eq. (1). Again the solution of Eq. (1)

consists of the yield penetration length l_r, the bond plastification length l_p and the elastic bar length:

$For\ 0 \le x \le l_r$

$$\varepsilon(x) = \varepsilon(0) - \frac{4f_b^{res}}{E_{sh}D_b}x \tag{11}$$

$$s(x) = s_2 + 0.5(l_r - x)\left[\varepsilon(x) + \varepsilon_{sy}\right] \tag{12}$$

$$f_b(x) = f_b^{res} \tag{13}$$

$For\ l_r \le x \le l_r + l_p:$

$$\varepsilon(x) = \varepsilon_{sy} - \frac{4f_b^{max}}{ED_b}(x - l_r) \tag{14}$$

$$s(x) = s_1 + 0.5\left(l_r + l_p - x\right)\left[\varepsilon(x) + \varepsilon_{el}^3\right] \tag{15}$$

$$f_b(x) = f_b^{max} \tag{16}$$

$$\varepsilon_{el}^3 = \varepsilon_{sy} - \frac{4f_b^{max}}{ED_b}l_p \tag{17}$$

For $l_r + l_p \le x \le \ell_D$:

$$\varepsilon(x) = C_1 \cdot e^{-\omega\left(x - l_p - l_r\right)} + C_2 \cdot e^{\omega\left(x - l_p - l_r\right)} \tag{18}$$

$$C_1 = \frac{\varepsilon(\ell_D) - \varepsilon_{el}^3 \cdot e^{\omega(\ell_D - l_p - l_r)}}{e^{-\omega(\ell_D - l_p - l_r)} - e^{\omega(\ell_D - l_p - l_r)}} \quad \text{and } C_2 = \varepsilon_{el}^3 - C_1 \tag{19}$$

$$s(x) = \frac{1}{\omega}\left(C_1 \cdot e^{-\omega\left(x - l_p - l_r\right)} - C_2 \cdot e^{\omega\left(x - l_p - l_r\right)}\right) \tag{20}$$

$$f_b(x) = \frac{f_b^{max}}{s_1} \cdot s(x) \tag{21}$$

The length of yield penetration l_r may be estimated if continuity of strain is considered at $x = l_r$, as

$$l_r = \left(\varepsilon(0) - \varepsilon_{sy}\right) \cdot \frac{E_{sh}D_b}{4f_b^{res}} \tag{22}$$

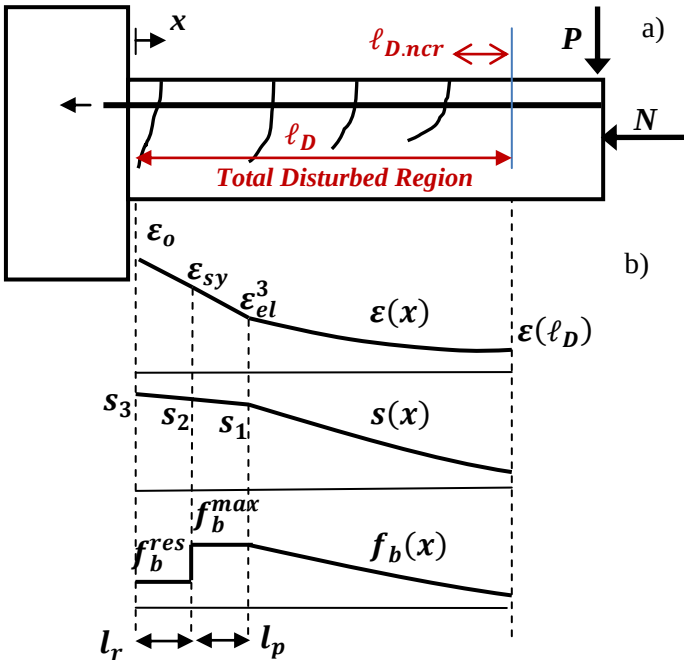

Figure 3: a) Definition of the ongoing development of the disturbed region. b) Plastic tensile bar response in the shear span of a cantilever RC column.

Equation (22) for the yield penetration length, common for the anchorage and the disturbed region, defines the plastic hinge having two interesting implications: first, it is a strain-based criterion for the spread of yielding in the shear span, as opposed to the stress-based definition given by Eq. (1a); there the coefficient *a* refers to the flexural overstrength normalized by the yielding moment.

A second more subtle point is the observation that the plastic hinge length is influenced by several parameters indirectly, through the determining effect that these have on f_b^{res}. For example the presence of axial load on a member that undergoes cyclic displacement reversals weakens the cover over a larger portion of the shear span length leading to cover delamination due to excessive compressive strains; upon reversal of load, the crushed cover cannot support significant bond action for the reinforcement when it is stressed in tension, leading to a reduced value of f_b^{res}, which in turn causes increased penetration depth for columns carrying a higher axial load; this is consistent with experimental reports.

3.1 Empirical relationships for plastic hinge length

The plastic hinge length ℓ_{pl} is defined in the literature as the length over which the flexural moments exceed the yielding capacity: $\ell_{pl} = (M_u - M_y) \cdot L_s / M_u$ (M_u is the ultimate moment and M_y is the yielding moment). However this theoretical definition does not comply with the experimental evidence; it is inconsistent too, since it would lead to a zero plastic hinge length region in the absence of hardening (when $M_y = M_u$). The plastic hinge length measured from the critical section towards the shear span signifies the region where intense inelasticity occurs during the earthquake. Despite the shortcomings associated with the mathematical definition of ℓ_{pl}, it was considered as a convenient artifact in earthquake engineering, necessary in order to conduct calculations of plastic rotation capacity due to flexure (according with $\theta_{pl} = (\varphi_u - \varphi_y) \cdot \ell_{pl}$ [10], θ_{pl} is the plastic rotation and φ_u, φ_y is the ultimate and yielding curvature). To avoid the inaccuracies associated with the mathematical expressions above, ℓ_{pl} is determined in design code procedures through calibrated empirical relationships that account primarily for the length of the shear span and the diameter of primary reinforcing bars (Eq. (23) [11], Eq. (24) [10], *h* = depth of the member):

$$\ell_{pl} = 0.08 \cdot L_s + 0.022 \cdot D_b \cdot f_y \tag{23}$$

$$\ell_{pl} = 0.1 \cdot L_s + 0.17 \cdot h + 0.24 \cdot D_b \cdot f_y / \sqrt{f_c} \tag{24}$$

In the context of the present paper, the length of plastic hinge is by definition the length of yield penetration (thus $\ell_{pl} = l_r$, l_r from Eq. (22)), occurring from the critical section towards the shear span; physically it refers to the extent of the nonlinear region and it may be used to calculate the inelastic rotation capacity of the column in the critical section. Contrary to the fixed design values adopted by codes of assessment, the former is actually the only consistent definition of the notion of the plastic hinge length.

4. MODEL VERIFICATION AND PARAMETRIC SENSITIVITY

The solution algorithm developed is applied in this section in order to establish the parametric sensitivities of the estimated plastic hinge to the important design parameters. As a reference point of the parametric analysis, which follows is the column experiment U3 [14]. The column specimen was tested as cantilever, simulating half a clear column length under lateral sway such as would occur during an earthquake with cross section detailing as shown in Fig. 4a. The specimen had a 350 mm square cross section reinforced with eight evenly distributed longitudinal reinforcing bars of D_b=25mm and stirrups of $D_{b,st}$=10mm spaced at 75mm o.c.

(on centers) and clear cover C_{cov}=32.5mm (*i.e.*, d=350-45=305mm). Concrete strength was f_c'=34.8MPa. Longitudinal steel yielding strength was 430MPa with a 5% hardening. Stirrup yield strength was 470MPa. Column shear span was L_s=1.0m and the axial load ratio [$\nu=N/(f_c' bd)$] was 0.16. Figure 4b plots the unified M-ϕ-ε relationship obtained for this axial load using fiber section analysis with the modified Kent & Park model for confined concrete [15]; a Hognestad-type parabola was used to model the compression stress-strain response of unconfined concrete [16]. Bond strength was taken equal to $f_b^{max}=1.25\sqrt{f_c'}$ (7.4MPa) for the anchorage (anchorage with a hook having an equivalent straight length of L_b=800mm). For the shear span the bond strength was calculated using a frictional model [32] that accounts for separate contributions of the cover concrete and stirrups as f_b^{max} =7.2MPa which drops to 2.75MPa after cover delamination. Due to the reversed cyclic nature of the displacement history, cover on the tension reinforcement is assumed to have delaminated or split if during the opposite direction of loading the compressive strain has attained the limit value of 0.004. The residual bond strength f_b^{res} is defined as 20% of the maximum bond strength and parameter s_1 = 0.2mm; s_2 mainly depends on the anchorage length which is equal to the shear span if the latter is transmitted to total disturbed region. For the present problem, s_2 is found equal to 0.5mm at the ultimate state of reinforcement (see Fig. 6a).

After evaluation of the process of crack formation according with the proposed algorithm, the resulting distribution of strains is illustrated in Fig. 5. Note that stabilization of cracking occurred before yielding of the tensile bars (just after formation of the 4th crack). Ultimate strain corresponded to a disturbed region extending over the entire length of the column shear span including an equivalent additional length equal to 12.5D_b (313 mm) – thus $\ell_{Do}^{max}=L_s+12.5D_b$– in order to account for the end detail of reinforcement at the tip of the column being welded on a steel plate (this additional length is the anchorage length equivalent of a T-headed anchorage– here this is a conservative estimate).

From Figure 5d it is seen that the yield penetration length over the shear span at the last step of the calculation was 319mm (0.91h or 0.32L_s) whereas the corresponding pullout slip was $s_u^{span}(x=0)$=2.36mm. When including the yield penetration in the footing as is intended in the formal definition of ℓ_{pl} (Eq. 22) - the total plastic hinge length is 632mm. (Note that the

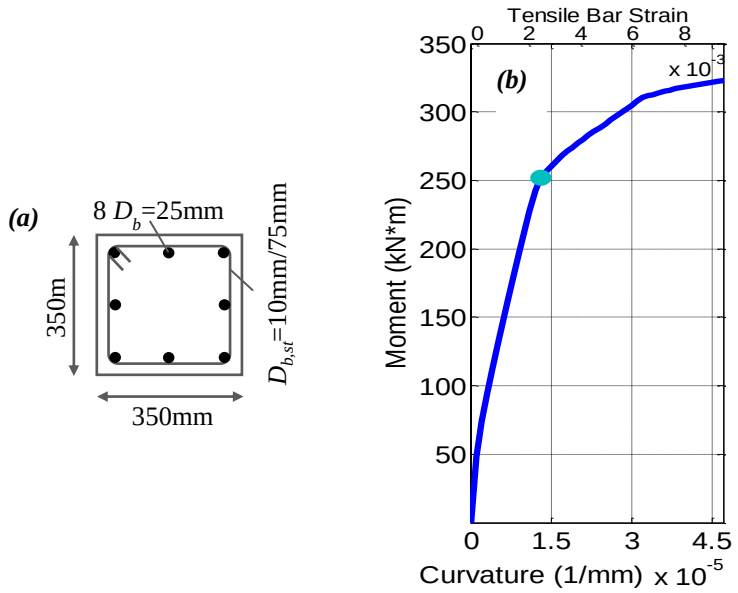

Figure 4: Specimen U3 a) cross section details, b) moment - curvature - tensile bar strain diagrams.

yield penetration length inside the footing is 313mm or $0.029D_b f_y$ and the corresponding slip is $s_u^{anch}(x=0)$=2.33mm.) Figure 6b compares this value with the empirical estimates of Eq. (24); the easy estimate of *0.5d* is also noted. Also included is the result of the classical definition of plastic hinge length $(1-M_y/M_u)L_s$. For comparison it is noted (red dashed line in Fig. 6b) that cover delamination extended over 520mm measured from the face of the support, according with the experimental report of specimen U3 [14].

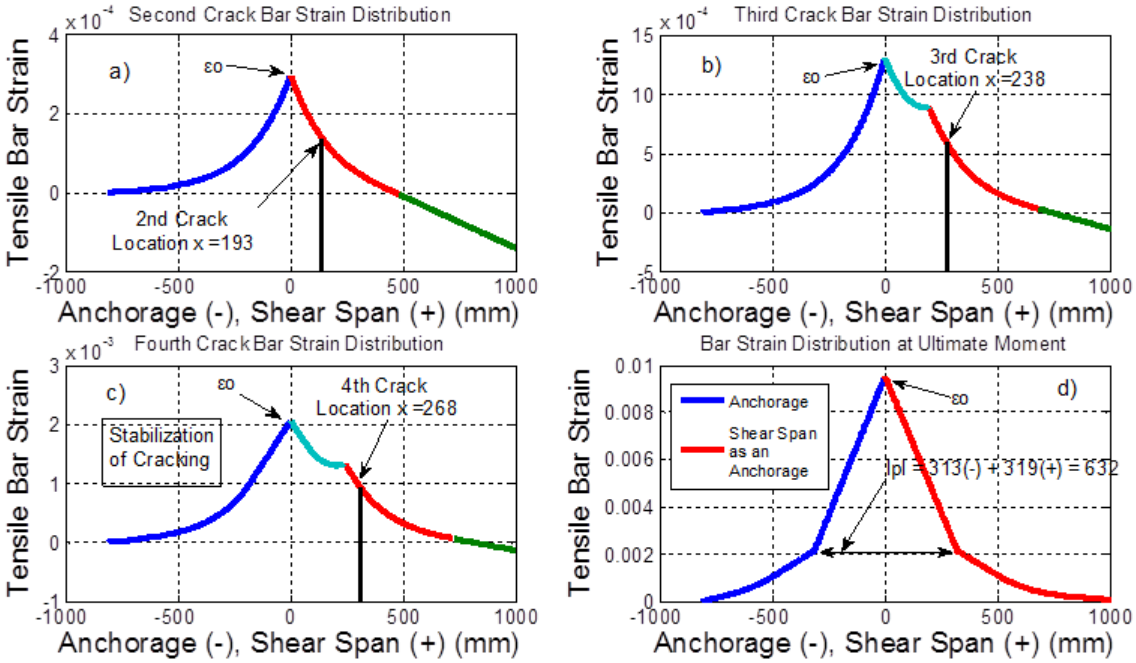

Figure 5: Column U3 (a), (b) (c) tensile bar strain distributions along the anchorage (blue curves) and the shear span (cyan-red-green curves). Location of estimated successive cracks is indicated until crack stabilization. d) Strain state of reinforcement at ultimate, where ℓ_{pl} is calculated.

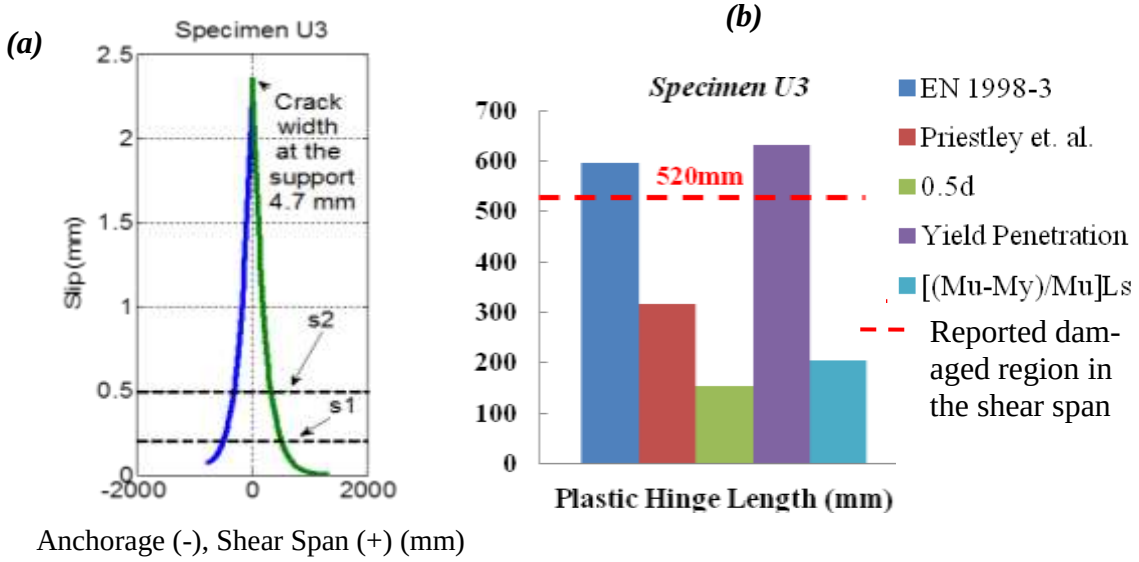

Figure 6: For specimen U3 a) slip distributions along the bar length at ultimate strain (where ℓ_{pl} is calculated) and b) analytical calculation of the plastic hinge length ℓ_{pl} (purple bar) and its correlation with the design equations.

Next a sensitivity analysis of the model is illustrated, using the column analyzed in the preceding as a reference case: the parameters studied were the applied axial load v (0.15, 0.3 and 0.5), the bond strength (3, 5, 7 MPa), the residual bond strength f_b^{res} (1, 2, 3MPa), the hardening modulus E_{sh} (1, 2.5 and 5% of E_s), the shear span length L_s (2, 3 and 4 times the section height h) and the bar size D_b (25 and 18mm), all included in Table 1. In each case one parameter is varied at a time keeping the reference values for all other variables constant (so the possible interaction effects between variables have not been considered in conducting the sensitivity analysis).

Parameter	**values**		
Axial load: $\nu=N/(f_c' bd)$	0.15	0.3	0.5
Bond strength, f_b^{max}	3	5	7
Residual bond strength, f_b^{res}	1	2	3
Hardening modulus, E_{sh}	1%	2.5%	5%
Shear span, L_s	2h	3h	4h
Bas size, D_b	25		18

Table 1: Parametric Investigation – Properties similar to specimen U3 (units: mm, MPa)

Figure 7a portrays the influence of the variables on the plastic hinge length of the reference specimen, as well as on the associated reinforcement tensile strain capacity of the critical cross section. Each curve in these diagrams is read as follows:

- Reducing the bond strength f_b^{max} (the associated residual value is $f_b^{res}=20\% f_b^{max}$) gradually from 7 to 3MPa (red arrow next to the brown curve pointing down) results in the increase of the plastic hinge length attained at lower bar strain,
- Increasing the axial normalized load v (red arrow next to light blue curve pointing up) lowers the strain capacity and the associated hinge length,
- Increasing the hardening modulus E_{sh} (red arrow next to green curve pointing up) increases the plastic hinge length and reduces the strain (as is implied by Eq. (22)),
- Increasing the bar size D_b (red arrow next to dark blue curve pointing up) increases the hinge length and reduces the strain (as is implied by Eq. (22)).
- The hinge length is relatively insensitive to L_s/h at low axial loads (all points coincide with the reference point (intersection of all curves; i.e. for L_s/h= 2, 3 and 4 the ℓ_{pl}/h is 1.8 and the associated strain is 0.017).

As was noted previously, the presence of axial load on a member that undergoes cyclic displacement reversals weakens the cover over a larger portion of the shear span length speeding up cover delamination due to excessive compressive strains; upon reversal of load, the crushed cover cannot support significant bond action for the reinforcement when it is stressed in tension, leading to a reduced value of f_b^{res}, which in turn causes increased penetration depth for columns carrying a higher axial load; this is consistent with experimental reports. Based on this experimental response, Fig. 7b depicts the effect of the studied variables on the hinge length when the axial load is relatively high (v=0.5) (in the reference case term f_b^{max} was reduced from 7.2MPa to 2.75 after cover loss):

- Reducing bond strength f_b^{max} from 7 to 3MPa (blue curve in Fig. 7b) results in increased plastic hinge length, attained at a higher bar strain,

- Reducing the residual bond strength f_b^{res} (orange curve in Fig. 7b) increases the hinge length and lowers the associated strain capacity.
- higher hardening modulus E_{sh} (green curve in Fig. 7b) increases the hinge length and also the strain.

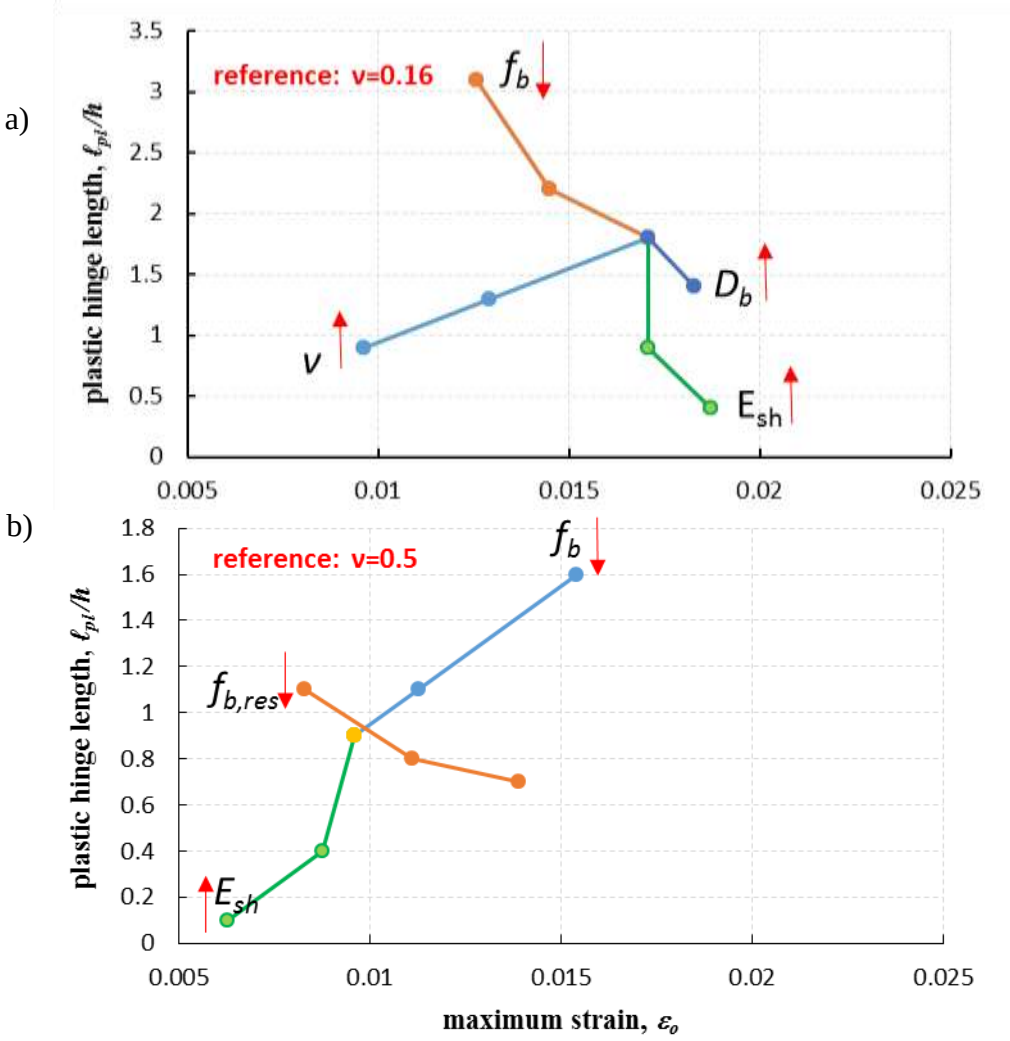

Figure 7: Sensitivity analysis (neglecting interactions): diagrams of normalized plastic hinge length to the cross section height versus the associated reinforcement maximum tensile strain for a) low (v=0.16) and b) high (v=0.5) axial load.

CONCLUSIONS

- Yield penetration occurs from the critical section towards both the shear span and the support of columns; physically it refers to the extent of the nonlinear region and determines the pullout slip measured at the critical section.
- Contrary to the fixed design values adopted by codes of assessment, the yield penetration length is actually the only consistent definition of the notion of the plastic hinge length, whereas the latter determines the contribution of pullout rotation to column drift and column stiffness.

- In order to establish the plastic hinge length in a manner consistent to the above definition, this paper pursued the explicit solution of the field equations of bond over the shear span of a column.
- Through this approach, the bar strain distributions and the extent of yield penetration from the yielding cross section towards the shear span were resolved and calculated analytically.
- By obtaining this solution a consistent definition of plastic hinge length is established, by reference to the state of reinforcement strain (replacing the stress based definition used previously).
- The true parametric sensitivities of this design variable for practical use in seismic assessment of existing structures are illustrated.
- The numerical results show good agreement with the experimental evidence and are consistent with the experimental trends supported by test databases, confirming that the plastic hinge length is controlled by the residual bond that may be mobilized along the yielded reinforcement.

ACKNOWLEDGEMENTS

The first author would like to thank the Alexander S. Onassis Public Benefit Foundation whose financial support is greatly appreciated.

7. References

[1] Syntzirma D. V., Pantazopoulou S. J. and Aschheim M. (2010), Load history effects on deformation capacity of flexural members limited by bar buckling. ASCE, Journal of Structural Engineering,136 (1),1−11.

[2] Bigaj A.J. (1999). Structural Dependence of Rotation Capacity of Plastic Hinges in RC Beams and Slabs PhD Thesis, Faculty of Civil Engineering, Delft University of Technology, Delft, The Netherlands.

[3] Bonacci, J., Marquez, J. (1994). Tests of Yielding Anchorages under Monotonic Loadings. ASCE, Journal of Structural Engineering, 120(3), 987-997.

[4] Tastani, S. P., and Pantazopoulou, S. J. (2013). Reinforcement and concrete bond: State determination along the development length. ASCE, Journal of Structural Engineering, 139(9), 1567−1581.

[5] Tastani, S. P., Brokalaki E., Pantazopoulou, S. J. (2015). State of Bond along Lap Splices. ASCE, Journal of Structural Engineering, 141(10), 04015007.

[6] Filippou, F., Popov, E., and Bertero, V. (1983). Modeling of R/C joints under cyclic excitations. ASCE, Journal of Structural Engineering, 109(11), 2666–2684.

[7] Tassios, T. P., and Yannopoulos, P. J. (1981). Analytical studies onreinforced concrete members under cyclic loading based on bond-sliprelationships. ACI Materials Journal, 78(3), 206-216.

[8] Tastani S.P., Pantazopoulou S.J. (2013). Yield penetration in seismically loaded anchorages: effects on member deformation capacity. Techno press Earthquake and Structures, 5(5):527-552.

[9] Tastani S.P, Thermou G.E., Pantazopoulou S.J. (2012). Deformation analysis of reinforced concrete columns after repair with FRP jacketing. 15th World Conference on Earthquake Engineering, September 24-28, Lisbon, Portugal (paper no. 3164).

[10] Eurocode 8, (2005). Design of structures for earthquake resistance − Part 3: Assessment and retrofitting of buildings , European Committee for Standardisation.

[11] Priestley, M.J.N., Seible F., and Calvi M. (1996). Seismic Design and Retrofit of Bridges. J. Wiley & Sons Inc., N. York.

[12] Scott, B.D., Park, R., and Priestley, M.J.N. (1982). Stress-strain behavior of concrete confined by overlapping hoops at low and high strain rates. J. American Concrete Institute, 79, 13-27.

[13] Fib Model Code (2010), Chapter 6:Interface Characteristics, Ernst & Sohn Publications, Berlin, Germany, pp.434.

[14] Saatcioglu M., and Ozcebe G. (1989). Response of Reinforced Concrete Columns to Simulated Seismic Loading. ACI Structural Journal, 86(1), 3-12.

[15] Scott, B.D., Park, R., and Priestley, M.J.N. (1982). Stress-strain behavior of concrete confined by overlapping hoops at low and high strain rates. J. *American Concrete Institute*, **79**, 13-27.

[16] Hognestad, E. (1951). *A Study of Combined Bending and Axial Load in Reinforced Concrete Members*. Bulletin No. 399, Engineering Experimental Station, University of Illinois.